JOURNAL OF MATERIALS SCIENCE 21 (1986) 1269–1274

Electrical properties of anodized aluminium in a humid atmosphere

YOSHIHIKO SADAOKA, YOSHIRO SAKAI, SHOJI MATSUMOTO
Department of Industrial Chemistry, Faculty of Engineering, Ehime University, Matsuyama 790, Japan

Complex impedance measurements have been made on porous anodized aluminium. The influence of humidity on electrical properties can be explained by an equivalent circuit based on the physical structure of the porous oxide film. The estimated resistance component decreases exponentially with humidity, while the humidity dependence of the two types of capacitance components cannot be confirmed below 80% r.h. Because the oxide film removes the barrier layer, a fair agreement between the impedance at 10^2 Hz and the resistance component of the pore sides is observed in humid atmospheres.

1. Introduction

The detection and control of humidity have recently become very important to human life, industrial equipment, etc. In humidity sensors using porous oxides, the impedance decreases by the physisorption and/or capillary condensation of water, and the humidity dependence of the impedance is strongly affected by the physical structure of the porous oxides [1–4].

In 1953, Ansbacher and Jason [5] reported that the electrical properties of anodized aluminium varied with the relative humidity in the atmosphere. Similar results were confirmed by many workers [6–9]. When aluminium is anodically oxidized in acid electrolytes in which the oxide is partially soluble, such as sulphuric acid, porous films are produced at low applied voltages. The film consists of a thin barrier layer adjacent to the metal and a thick outer layer. The porous layer consists of approximately hexagonally close-packed cyclindrical pores normal to the metal surface and extending to the outer surface. The thickness of the porous layer is easily controlled by the oxidation time at a constant current density, and the thickness of the barrier layer is controlled by the oxidation voltage.

While the structure of the pores of the sintered porous oxides is complex [4] and it is difficult to discuss, in detail, the effects of the adsorbed water on the impedance in humid atmospheres, the film of the porous oxide, prepared by anodic oxidation of aluminium, is favourable for studying these effects.

The results of the study of the humidity dependence of the impedance of anodically oxidized aluminium by the methods of complex impedance and admittance analyses are presented in this paper.

2. Experimental details

2.1. Sample preparation

High-purity aluminium plate (99.999%) was anodized in a 5 wt % sulphuric acid solution at constant current density ($10\,\mathrm{mA\,cm^{-2}}$) and followed by potentiostatical reanodization in a 2 wt % ammonium borate solution at room temperature. The reanodization voltage varied from 20 to 350 V. The oxide layer thus obtained (a transparent sheet) was washed and then dipped into distilled water for 30 min in order to eliminate the residual electrolyte. The film was dried in oxygen at 200° C. A gold electrode ($0.4 \times 0.4\,\mathrm{cm^2}$) was deposited under vacuum on the film formed on the aluminium. The aluminium base was used as a counter electrode.

In addition, the oxide film removed the barrier layer and the aluminium base was prepared by the following procedures: first, the oxide film was removed from the base by reverse electrolysis in sulphuric acid solution. Second, the barrier layer of the oxide film was removed by chemical etching with 5 wt % sulphamic acid solution at 70° C [10]. The gold electrodes ($0.2 \times 0.2\,\mathrm{cm^2}$) were deposited under vacuum on both surfaces of the oxide film which removed the barrier layer.

2.2. Measurements

Pore-size distribution was examined by means of mercury penetration porosimetry. The surface area was measured using nitrogen and water as adsorbates. The amount of water adsorbed was measured using a quartz spring balance as follows: the vessel containing the oxide film was evacuated to below 10^{-1} torr followed by the slow introduction of water vapour or the evacuation of vapour. The oxide film was allowed to stand in the vessel until the weight became constant. The oxide film for the previously mentioned analyses was prepared by peeling the oxide from the aluminium base by inverse electrolysis in a sulphuric acid solution.

Humidity–impedance characteristics were measured using impedance meters (Hewlett Packard, 4276A and 4277A) from 10^2 to 10^6 Hz. Humidities (% r.h.), ranging from 0 to 90, were prepared by mixing dry and moist air in controlled proportions at 30° C.

0022–2461/86 $03.00 + .12

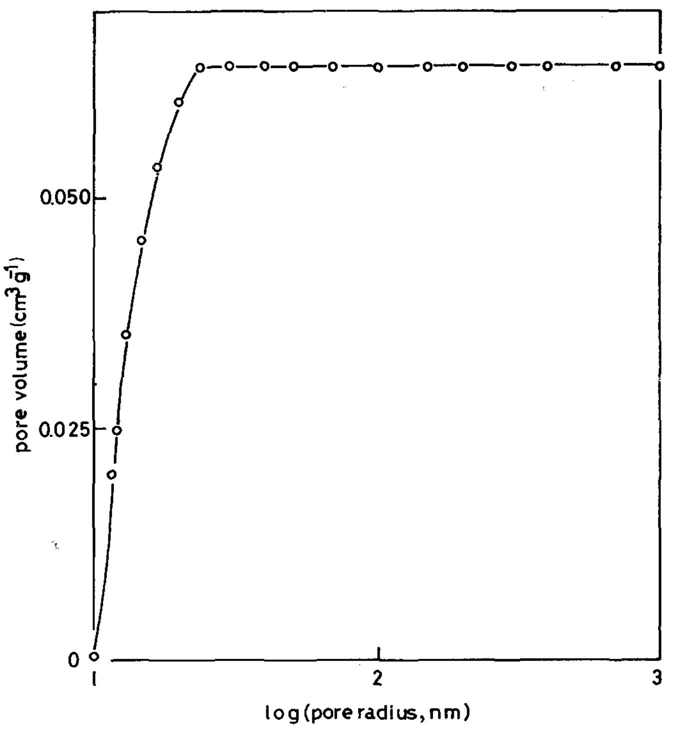

Figure 1 Pore size distribution curve obtained by use of the mercury porosimeter.

3. Results and discussion

3.1. Pore structure and adsorption of water

Fig. 1 shows the accumulated pore distribution curve. The volumes of pores smaller than 30 nm in pore radius is 0.064 cm^3 g^{-1}. Pores larger than 30 nm radius are not likely to exist. As previously mentioned, the oxide film prepared by anodic oxidation in sulphuric acid solution consists of a thin barrier layer adjacent to the metal, and a thick outer porous layer. For a thin film prepared by anodic oxidation in 5 wt % sulphuric acid solution at 10 mA cm^{-2} for 20 min, the thickness of the total oxide layer is estimated to be 6.2 μm from the capacitance measurement in a dry atmosphere, and the thickness of the barrier layer to be $\sim$ 18 nm. This was calculated by using the approximation of 1 nm V^{-1} of applied voltage for films in sulphuric acid [11]. In addition, it seems that the porous layer consists of hexagonally close-packed cylindrical pores, with an average pore diameter of 18 nm [8], a distance of 46.8 nm between two adjacent pores [8], and an oxide density of 3.32 g cm^{-3} [6]. By using these values, the pore volume and the surface area of pore sides are estimated to be 0.045 cm^3 g^{-1} and 10 m^2 g^{-1}, respectively. These estimated values are comparable to the values obtained by mercury penetration porosimetry (0.064 cm^3 g^{-1}) and adsorption methods (17 m^2 g^{-1} using nitrogen as adsorbate and 12 m^2 g^{-1} using water as adsorbate). In addition, the cross sectional area of the pores is 14% of the superficial surface area.

The amount of adsorbed water at 95% r.h. is 0.060 g g^{-1} and comparable to the total volume of pores smaller than 30 nm radius as determined by mercury porosimetry. This agreement between the amount of adsorbed water at 95% r.h. and the pore volume indicate the possibility of capillary condensation in humid atmosphere. By using Kelvin's equation for capillary condensation, the maximum value of pore radius in which capillary condensation occurs can be estimated as a function of humidity. In Table I, the maximum value of pore radius, the pore volume determined by mercury porosimetry, and the amount of adsorbed water are summarized as a function of humidity. Above 90% r.h. the agreement between the amount of adsorbed water and the pore volume is confirmed. In this case, the density of the adsorbed water is assumed to be 1 g cm^{-3}. This agreement suggests that most of the adsorbed water exists in the capillary condensed water at 90% r.h. and above.

3.2. Electrical properties

3.2.1. Anodized film with barrier layer

The humidity dependence of impedance in the frequency range 10^2 to 10^6 Hz was measured at 30° C. The humidity dependence of the impedance at 10^2 Hz is shown in Fig. 2. The impedance decreases with humidity. In a humid atmosphere, the impedance increases with the reanodization voltage, but any similar dependence cannot be confirmed in a dry atmosphere. The frequency dependence of the impedance has been distinctly observed.

This frequency dependence indicates that the impedance consists not only of a resistance component but also a capacitance component. For example, the result of some complex impedance plots are shown in Fig. 3. In a dry atmosphere, a steep rise of the imaginary part of impedance was observed. The impedance is

TABLE I Characteristic values

r.h. (%)	Pore radius* (nm)	Pore volume† (cm^3 g^{-1})	W_{H_2O}‡ (g g^{-1})
85	6.8	–	0.022
90	10.5	0.010	0.033
92	13.3	0.035	0.036
95	21.7	0.064	0.060

*Kelvin's equation.
†Mercury penetration porosimetry.
‡Amount of adsorbed water.

inversely proportional to the frequency; therefore, the impedance consists only of a capacitance component. The estimated value of the capacitance is poorly dependent on the reanodization voltage and inversely proportional to the quantity of electricity in the anodizing procedure [8]. The capacitance, therefore, refers to the oxide layer.

In a humid atmosphere, the high-frequency results were represented by nearly perfect circular arcs; all of which passed through the origin, and a steep rise of the imaginary part was observed in the low-frequency region as shown in Fig. 3. For the film prepared at low reanodizing voltages, clear arcs were observed in humid atmospheres, but similar arcs could not be observed for the film prepared at reanodizing voltages above 100 V.

The observed frequency dependence of impedance can be represented by an equivalent circuit as shown in Fig. 4. The individual components are estimated by complex impedance and admittance analyses. The humidity dependences of the C_l and R_l components are shown in Fig. 5. The R_l component decreases exponentially with humidity and is poorly dependent on the reanodizing voltage. Furthermore, it is confirmed that the R_l component is linearly proportional to the anodizing time at constant current density.

Below 80% r.h., the C_l component is poorly dependent on the humidity and the reanodizing voltage and in fair agreement with the capacitance observed in a dry atmosphere. The C_l component observed at 90% r.h. is considerably larger than that observed at 80% r.h. and below. This increment may be

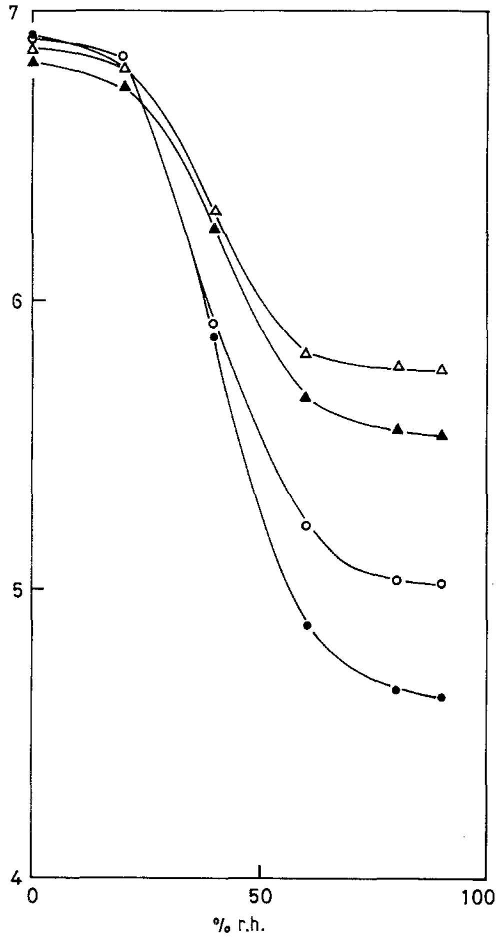

Figure 2 Humidity dependence of impedance at 10^2 Hz. Reanodization voltage: ●, 20 V; ○, 50 V; ▲, 200 V; △, 300 V.

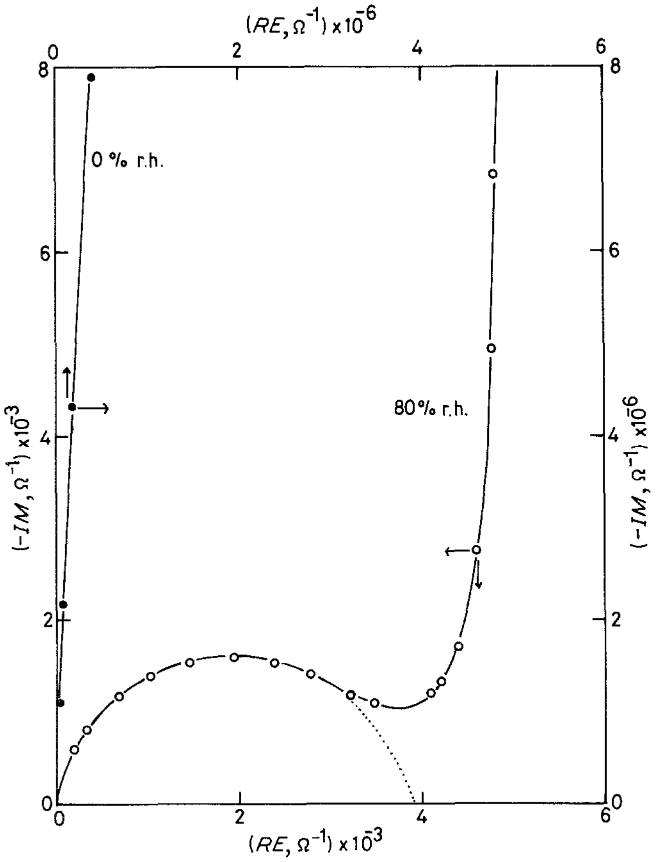

Figure 3 Complex impedance plots for the film reanodized at 20 V. Humidity (% r.h.) is shown in the figure.

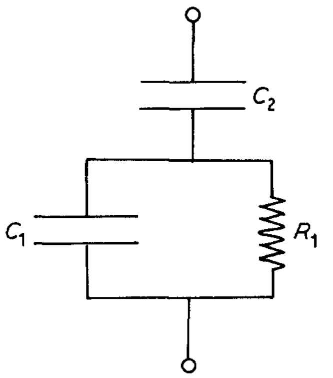

Figure 4 Equivalent circuit. C_2 and C_1 refer to the capacitance, R_1 refer to the resistance.

attributable to the capillary condensed water. By assuming that all of the adsorbed water exists as capillary condensed water within the cylindrical pores (pore length; 6.2 μm) and the dielectric constant of the condensed water is 80 at 90% r.h., the increment of the C_1 component caused by the condensed water can be estimated as a function of the effective electrode area of the dielectrics composed of condensed water as shown in Fig. 6. For the increment of the C_1 component at 90% r.h., the effective electrode area of the dielectrics is estimated to be $\sim 15\%$ of the gold electrode area. This estimated value is comparable to the cross-sectional area of pores as previously mentioned. In addition, the specific resistance of the capillary condensed water at 90% r.h. is estimated to be $\sim 4 \times 10^4\,\Omega$cm and comparable to that ($3.8 \times 10^4\,\Omega$cm) of water trapped from the air.

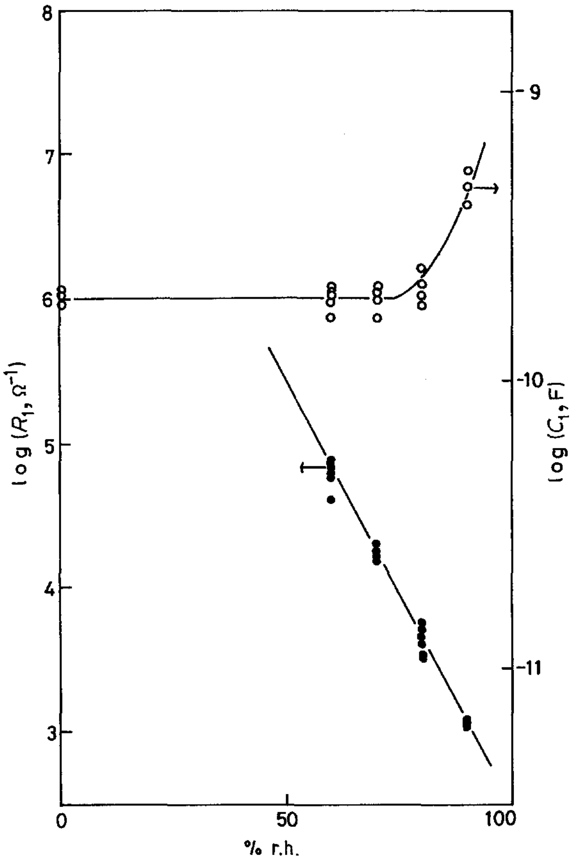

Figure 5 Humidity dependences of R_1 and C_1 for the films reanodized at various voltages.

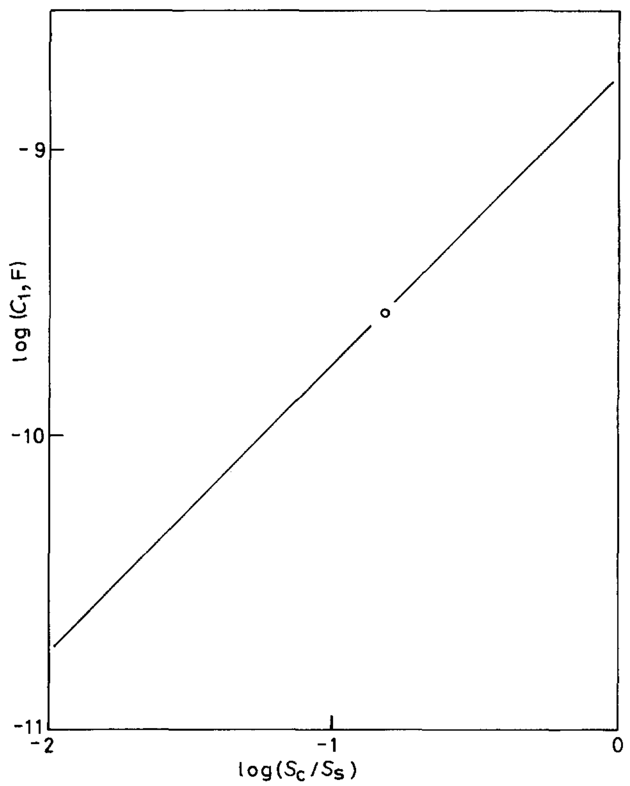

Figure 6 The relation of the increment of C_1 and the ratio of the cross-sectional area of pores, S_c, and the superficial surface area, S_s. ○, The observed increment of C_1 at 90% r.h.

While the R_1 and C_1 components are scarcely dependent on the reanodizing voltage, the C_2 component is inversely proportional to the reanodizing voltage and is poorly dependent on the humidity, as shown in Fig. 7. When aluminium is anodically oxidized in a solution in which the oxide solubility is very low, such as ammonium borate, adherent compact films of

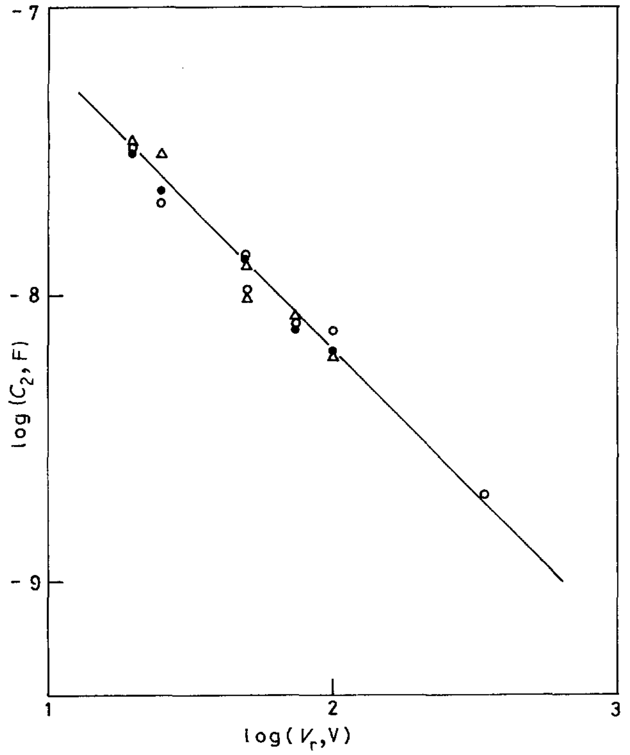

Figure 7 The reanodization voltage (V_R) dependence of C_2. ●, 90% r.h.; ○, 80% r.h.; △, 60% r.h.

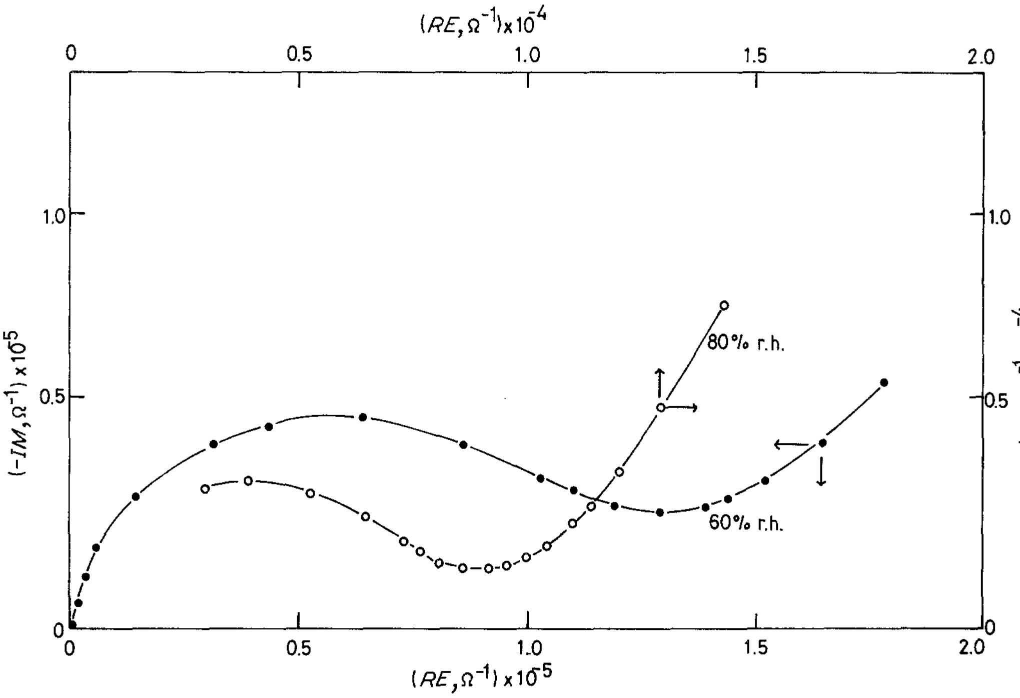

Figure 8 Complex impedance plots for the film which removed the barrier layer by chemical etching. Humidity is shown in the figure.

thickness ~ 1.4 nm V^{-1} of the anodizing voltage are produced [11]. It seems that the potentiostatic reanodization of the film prepared in a sulphuric acid solution leads to the development of a barrier layer adjacent to the metal. The reanodization has little influence on the structures of the preformed pore layer. Since the C_2 component is inversely proportional to the reanodizing voltage, it seems that the C_2 component refers to the barrier layer.

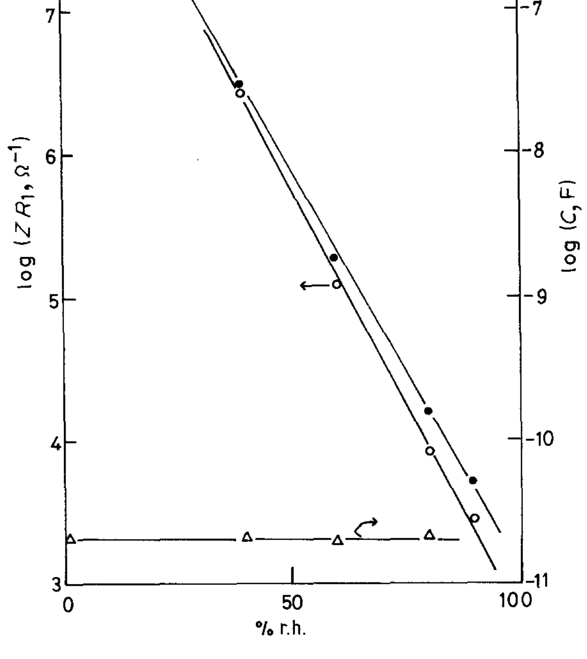

Figure 9 Humidity dependence of R_1, C_1, C_2 and Z at 10^2 Hz for the film which removed the barrier layer. △, C_1; ▲, C_2; ○, R_1; ●, Z.

While the exact surface area of the barrier layer cannot be determined, the surface area can be estimated by assuming the geometry of the barrier layer. For simplicity, two geometries of the barrier layer are considered. First, the surface of the barrier layer is flat and perpendicular to the direction of pore growth. For this model, the surface area of the barrier layer is approximately 14% of the superficial surface area. Second, the barrier layer is formed in a hemisphere. In this case, the surface area of this layer is approximately 93% of the superficial surface area. As in the results, the thickness of the barrier layer is estimated to be 0.27 nm V^{-1} of the reanodizing voltage for the former case and 1.78 nm V^{-1} for the latter case. These estimations convinced us that the C_2 component obtained from the complex impedance analyses refers to the capacitance of the barrier layer adjacent to the metal.

From the observed results, it was concluded that C_2 refers to the barrier layer of oxide, and C_1 refers to the sum of the porous outer layer of oxide and the capillary condensed water. R_1 refers to the pore sides and decreases exponentially with increases in humidity. In addition, it is realized that the minimum values of the impedance in Fig. 2 are restricted by the thickness of the barrier layer.

3.2.2. Anodized film removed the barrier layer

Complex impedance plots are shown in Fig. 8. In humid atmospheres, the high frequencies are represented by nearly perfect arcs, all of which pass through the origin. A "spur" was observed in the low-frequency region. It is confirmed that the frequency dependence can be represented by the equivalent circuit showed in Fig. 4. In the low-humidity region, the estimation of the C_2 component was incorrect, but the C_1 and R_1 components can be estimated from the complex impedance and/or admittance analysis. The humidity dependences of C_1 and R_1 are shown in Fig. 9. While the C_1 component is poorly dependent on the humidity, the R_1 component decreases exponentially with increase in humidity and the slope of the line in the plot of log R_1 against humidity is comparable to that shown in Fig. 5. The total thickness of this film and the superficial electrode area were determined to be 19 μm and 0.04 cm^2, respectively, from a micrometer and cathetometer measurements. For $C_1 = 20$ pF, $\varepsilon = 8.8$ and the electrode area is 0.04 cm^2, the thickness of the oxide layer is estimated to be 15.6 μm. In addition, the thickness of the porous layer is estimated to be 18.6 μm from the anodizing time at the constant current density of 10 mA cm^{-2}. The values obtained indicate that the C_1 component refers to the capacitance of the porous oxide layer. On the other hand, the C_2 component, $\sim 1.3\,\mu$F, obtained in humid atmospheres is much larger than that of the oxide films with a barrier layer. By assuming that the C_2 component refers to the barrier layer and the electrode area of this layer is 93% of the superficial surface area, the thickness of this layer is estimated to be ~ 0.22 nm. This value for the thickness of the barrier layer is extremely small. It seems that the C_2 component refers to the electrode polarization and the barrier layer is completely removed by chemical etching. The fair agreement between the impedance at 10^2 Hz and the R_1 component is confirmed for the oxide film's removal of the barrier layer in a humid atmosphere, and the humidity dependence of the impedance is enhanced by the removal of the barrier layer. This improved dependency is preferable for films used as humidity sensors.

It is concluded that the electrical properties of an anodized aluminium can be explained by an equivalent circuit based on the physical structure of the porous oxide film. In previous papers [2–4, 8, 9, 12, 13] the effects of the physisorbed water on pore sides and/or the capillary condensed water in pores on the resistance component had been considered in detail on the basis of the results observed in many types of porous material. Hence, the detailed discussion of the R_1 component was omitted in this paper.

References

1. Y. SHIMIZU, H. ARAI and T. SEIYAMA, *Denki Kagaku* **50** (1982) 831.
2. Y. SADAOKA and Y. SAKAI, *ibid.* **51** (1983) 879.
3. *Idem, ibid.* **51** (1983) 873.
4. *Idem, Hyomen Kagaku* **5** (1984) 220.
5. F. ANSBACHER and A. G. JASON, *Nature* **171** (1953) 177.
6. A. C. JASON and J. L. WOOD, *Proc. Phys. Soc.* **B68** (1955) 1105.
7. A. FURUICHI, *Denkigakkai Ronbunshi* **A100** (1980) 39.
8. Y. SADAOKA and Y. SAKAI, *Denki Kagaku* **50** (1982) 172.
9. *Idem,* Proceedings of the International Meeting on Chemical Sensors, Fukuoka, September 1983, edited by T. Seiyama, K. Fueki, J. Shiokawa and S. Suzuki (Kodansha-Elsevier, 1983) p. 416.
10. H. AKAHORI, *Denshi Kenbikyo* **12** (1977) 21.
11. M. HUNTER and P. FOWLE, *J. Electrochem. Soc.* **101** (1954) 481.
12. Y. SADAOKA and Y. SAKAI, *Denki Kagaku* **51** (1983) 437.
13. *Idem, ibid.* **51** (1983) 285.

Received 29 April
and accepted 10 June 1985